Received: 30 July 2022 | Revised: 28 January 2023 | Accepted: 3 March 2023

DOI: 10.1111/cas.15783

Cancer Science WILEY

ORIGINAL ARTICLE

In vivo CRISPR screens identify RhoV as a pro-metastasis factor of triple-negative breast cancer

Ming-Liang Jin[1,2] | Yue Gong[1,2] | Peng Ji[1,2] | Xin Hu[1,3] | Zhi-Ming Shao[1,2,4]

[1]Department of Breast Surgery, Key Laboratory of Breast Cancer in Shanghai, Fudan University Shanghai Cancer Center, Fudan University, Shanghai, China

[2]Department of Oncology, Shanghai Medical College, Fudan University, Shanghai, China

[3]Precision Cancer Medicine Center, Shanghai, China

[4]Institutes of Biomedical Science, Fudan University, Shanghai, China

Correspondence
Xin Hu and Zhi-Ming Shao, Department of Breast Surgery, Key Laboratory of Breast Cancer in Shanghai, Fudan University Shanghai Cancer Center 270 Dong-An Road, Shanghai, 200032, PR China.
Email: xinhu@fudan.edu.cn and zhi_ming_shao@163.com

Funding information
China Postdoctoral Science Foundation, Grant/Award Number: 2022M710757; National Natural Science Foundation of China, Grant/Award Number: 81502278, 81572583, 82103369 and 82202995

Abstract

Metastasis is the main death reason for triple-negative breast cancer (TNBC). Thus, identifying the driver genes associated with metastasis of TNBC is urgently needed. CRISPR screens have dramatically enhanced genome editing and made it possible to identify genes associated with metastasis. In this study, we identified and explored the crucial role of ras homolog family member V (RhoV) in TNBC metastasis. Here, we performed customized in vivo CRISPR screens targeting metastasis-related genes obtained from transcriptome analysis of TNBC. The regulatory role of RhoV in TNBC was validated using gain- or loss-of-function studies in vitro and in vivo. We further conducted immunoprecipitation and LC–MS/MS to explore the metastasis mechanism of RhoV. In vivo functional screens identified RhoV as a candidate regulator involved in tumor metastasis. RhoV was frequently upregulated in TNBC and correlated with poor survival. Knockdown of RhoV significantly suppressed cell invasion, migration, and metastasis both in vitro and in vivo. In addition, we provided evidence that p-EGFR interacted with RhoV to activate the downstream signal pathway of RhoV, thereby promoting tumor metastasis. We further confirmed that this association was dependent on GRB2 through a specific proline-rich motif in the N-terminus of RhoV. This mechanism of RhoV is unique, as other Rho family proteins lack the proline-rich motif in the N-terminus.

KEYWORDS
CRISPR screen, EGFR, GRB2, invasion and metastasis, RhoV, triple-negative breast cancer

1 | INTRODUCTION

Triple-negative breast cancer (TNBC), which lacks the expression of estrogen receptor (ER), progesterone receptor (PR), and the amplification of human epidermal growth factor receptor 2 (HER2),[1] has the worst prognosis in all breast cancer subtypes. TNBC accounts for about 15% of breast cancer patients,[2] and shows a high metastasis rate, especially for internal organs, such as lung, brain, or liver.[3] Metastasis is the main death reason for TNBC patients,[4] and lung is the most common site of TNBC metastasis.[4,5] However, the underlying mechanism of TNBC

Abbreviations: CCLE, Cancer Cell Line Encyclopedia; DFS, disease-free survival; EGFR, epidermal growth factor receptor; FUSCC, Fudan University Shanghai Cancer Center; GRB2, growth factor receptor-bound protein 2; GTP/GDP, guanosine triphosphate/diphosphate; HER2, human epidermal growth factor receptor-2; JNK1/2, c-jun N-terminal kinase 1/2; MOI, multiplicity of infection; PAK1, p21 (RAC1) activated kinase 1; PBS, phosphate buffer solution; PCR, polymerase chain reaction; RhoV, ras homolog family member V; RTK, receptor tyrosine kinase; TCGA, The Cancer Genome Atlas; TNBC, triple-negative breast cancer.

Ming-Liang Jin, Yue Gong, and Peng Ji contributed equally to this work.

metastasis remains unclear. Moreover, biomarkers to identify TNBC patients with the highest risk is urgently needed.

CRISPR screens have dramatically enhanced genome editing and made it possible to identify novel cancer-associated genes.[6] In our study, we utilized CRISPR screening for metastasis-related genes and identified ras homolog family member V (RhoV) as a key factor involved in tumor metastasis. RhoV is a member of the Rho protein family. Early views believed Rho protein family played a role in regulating the organization of actin cytoskeleton, but it was not considered to be an oncogene.[7] However, this view is gradually changing. In recent years, studies have shown activation of Rho protein family is closely related to tumor formation.[8]

Rho family GTPase can regulate a variety of cell functions, including cytoskeleton formation, cell proliferation, and so on, all of which have been confirmed to be important for cancer.[9] Generally, Rho GTPases acts as a molecular regulatory switch in the form of active GTP binding, which enables Rho GTPases to interact with downstream molecules.[10] The conversion between the GTP-bound form and GDP-bound form is regulated by the guanine nucleotide exchange factors[11] and GTPase-activating proteins.[12]

In this study, we firstly identified RhoV as a key regulator of TNBC metastasis. It is worth noting that RhoV was found to be closely associated with poor clinical outcomes and to be an independent prognostic factor of TNBC. We found that the N-terminal extension of RhoV acts as a binding site of GRB2, physically linking RhoV to the epidermal growth factor receptor (EGFR). In addition, we demonstrated that the binding between RhoV and GRB2 is important for RhoV in regulating the EGF-induced cell migration.

2 | MATERIALS AND METHODS

2.1 | Human cancer cell lines

We used human cell lines BT-549, HCC-70, Hs-578T, MDA-MB-231, LM2-4175, Hela, and HKT-293T (from American Type Culture Collection, ATCC). The identity of each cell line was verified by analysis of short tandem repeats. As mentioned previously, the cells were grown in fully grown medium.[13] All cell lines were cultured in a humidified incubator at 37°C and 5% CO_2. The human TNBC cell line transcriptome data were obtained from the Cancer Cell Line Encyclopedia (CCLE) portal (https://portals.broadinstitute.org/ccle).[14]

2.2 | Animal models

For animal experiments, we followed the NIH Guide for the Care and Use of Laboratory Animals. In our research, 7- to 8-week-old female NOD/SCID mice (GemPharmatech LLC.) were used in all animal models. For mouse tail vein metastasis assays, 1×10^6 cells transfected with metastasis-related gene library were injected into NOD/SCID mice. The fluorescence method was utilized to image tumor in mice to observe the status of tumor metastasis. After 6 weeks, the mice were sacrificed.

2.3 | RNA-Seq data analysis and metastasis-related gene analysis

Based on 360 cases of the primary TNBC transcriptome database from Fudan University Shanghai Cancer Center (FUSCC), samples were divided into four subtypes.[15] Within the four TNBC subtypes, samples were further divided into a high-risk group that has metastasis within 3 years and a low-risk group that has no metastasis within 3 years. The differentially expressed genes were analyzed between the two groups using DESeq2. Genes with a fold change (FC) value greater than 1.5 and *t*-test *p*-value less than 0.05 were selected as differentially expressed genes.

2.4 | Virus production and infection

We transfected pWPXL-GFP-luc, psPAX2, and pMD2G plasmids into HEK293T cells for lentivirus generation. Forty-eight hours after virus transfection, cells were sorted by flow cytometry based on GFP-labeled fluorescence. After that, we applied lentiCas9-Blast, psPAX2, and pMD2G plasmids for lentivirus generation. Forty-eight hours after virus transfection, 5 μg/mL blasticidin was used to select stably integrated cells for 6 days.

The primer sequence for sgRNA generation was obtained from http://www.addgene.org/pooled-library/zhang-human-gecko-v2/, and purified subsequently by RNase-free HPLC (Table S1). After primer annealing, a sgRNA was copied into one lentiGuide-puro plasmid. LentiGuide-puro plasmids containing all sgRNAs were mixed together. The metastasis-related library virus mixture was generated in HEK293T cells. Then, target cells with Cas9-GFP-luciferase were infected by library viruses related to metastasis in a low multiplicity of infection (MOI = 0.3) to make sure most cells receive one sgRNA plasmid. Forty-eight hours after infection, cells were selected with puromycin in 1 μg/mL for 5 days.

2.5 | DNA extraction and sgRNA readout

To evaluate the expression of sgRNA, we applied next-generation sequencing (NGS). The QIAamp DNA Mini Kit (Qiagen) was applied to extract genomic DNA (gDNA) from xenografts and cells. As mentioned earlier, the two-step PCR procedure was used to amplify the sgRNA library of each sample, and the samples were prepared for Illumina sequencing.[16]

2.6 | sgRNA data analysis

The original FASTQ data were processed with Geneious 7.0 (Biomatters). We applied the "map to reference" function in Geneious 7.0 to assemble the reads into reference sequence. After matching, the number of reads for each library barcode was counted. The number of readings for each sample was normalized

as follows: normalized reading count for each unique barcode reading/total reading for all barcodes in the sample$\times 10^6 + 1$. Then, we used the Model-based Analysis of Genome-wide CRISPR/Cas9 Knockout (MAGeCK) algorithm to quantify the enrichment of candidate genes.[17] Negatively screened genes were defined as genes with decreased barcodes. The mScore of genes was calculated as follows: sum of -$\log_{10}$ (p-value) of genes resulting from the MAGeCK algorithm.

2.7 | Expression plasmids

We purchased pENTER-RhoV (CH883195) and pENTER-GRB2 (CH895066) plasmids from Vigene Biosciences. To construct RhoV activation mutation RhoV G40V and RhoV SH3-binding site mutations Mut1, Mut2, Mut3, Mut4, and Mut5, we utilized the Mut Express II Fast Mutagenesis Kit V2 (Vazyme, C214-01) to complete plasmid construction.

2.8 | Western blotting

Tissue protein extraction reagent (Thermo Fisher Scientific) was used to obtain whole cell extracts with protease and phosphatase inhibitors. Then, the cell lysate was dissolved in 5×SDS-PAGE loading buffer and boiled for 10 min. The proteins were next splitted by SDS-PAGE gel and transferred on a polyvinylidene fluoride membrane (Roche). The membrane was blocked with 5% BSA in TBST solution for 60 min. Next, we utilized the primary antibody to blot at 4°C for 12–16 h: rabbit polyclonal anti-HA (Cell Signaling Technology [CST]; 1:1000, no.3724), mouse polyclonal anti-GAPDH (ProteinTech; no.60004-1-Ig, 1:5000), mouse polyclonal anti-Vinculin (ProteinTech; no.66305-1-Ig, 1:5000), rabbit polyclonal anti-Flag (Sigma; no. F7425, 1:1000), rabbit polyclonal anti-PAK1 (CST; catalog no.2602, 1:1000), mouse polyclonal anti-β-Actin (CST; no.4970, 1:5000), rabbit polyclonal anti-His (ProteinTech; Cat No. 66005-1-Ig, 1:1000), rabbit polyclonal anti-GRB2 (ProteinTech; Cat No. 10254-2-AP, 1:1000), rabbit polyclonal anti-EGFR (CST; no.4267, 1:1000), and rabbit polyclonal anti-Phospho-EGFR (CST; no.4267, 1:1000). After washing with TBST three times, the membrane was incubated for 60 min at room temperature with HRP-conjugated goat anti-mouse antibody (Jackson ImmunoResearch; 1:5000) or goat anti-rabbit antibody (Jackson ImmunoResearch; 1:5000), and proteins were detected with chemiluminescence substrate (Thermo Fisher Scientific). The image system was Molecular Imager ChemiDocXRSþ.

2.9 | Cell viability analysis

Cells were seeded in 100 μL of their corresponding growth medium using 2000 cells per well in 96-well plates in triplicate, and cell viability was determined by Cell Counting Kit-8 (CCK-8) (Vazyme, A311-01). The absorbance was measured at 450 nm.

2.10 | Transwell assay

We resuspended the cells with serum-free medium to the top compartment of the transwell chamber (migration chamber Corning #353097; invasion chamber Corning #354480), and 600 μL of medium was added with 10% fetal bovine serum to the bottom chamber. For migration assays, all cell lines were cultured in a humidified incubator at 37°C and 5% CO2 and allowed migration for 12 h (MDA-MB-231), 7 h (BT-549), or 48 h (HCC-70). For invasion assays, all cell lines were allowed migration for 24 h (MDA-MB-231), 14 h (BT-549), or 72 h (HCC-70). After removing nonmigrated cells, cells were stained with crystal violet.

2.11 | Wound-healing assay

The MDA-MB-231, HCC-70, and BT-549 cells were cultured in six-well dishes. When the cells reached 100% confluence, the cell monolayer was scratched with pipette tip. Then the dishes were washed twice with PBS and incubated with medium with 10% fetal bovine serum. All cell lines were cultured in a humidifified incubator at 37°C and 5% CO_2 and allowed migration for 24 h.

2.12 | Semiquantitative reverse transcription-polymerase chain reaction (RT-PCR)

For RT-PCR analysis, we used TRIzol (Invitrogen) to extract RNA from cells and PrimeScript RT Reagent Kit (TaKaRa) to transform RNA into cDNA following the manufacturer's protocol. TaKaRa-Ex-Taq (TaKaRa) was applied for PCR amplification. Samples were processed using the Applied Bioscience 7900HT Fast Real-Time PCR System. Specific primers for RhoV (5-CCTCATCGTCAGCTACACCTG-3; 5-GAACGAAGTCGGTCAAAATCCT-3) and GAPDH (5-GGAGCGAG ATCCCTCCAAAAT-3; 5-CCTTGCGCATCATGGTGTT-3) as reference gene primers were utilized.

2.13 | Immunoprecipitation (IP)

Hemagglutinin (HA) IP experiments were performed as previously described.[18] Cells were lysed in NP40 buffer (Beyotime Biotechnology) with protease and protein phosphatase inhibitors. IPs were also performed in NP40 buffer with anti-HA immune magnetic beads (Bimake, catalog no. B26202) and incubated overnight at 4°C.

2.14 | Proteomic analysis

HEK293T cells expressing pENTER and HA-RhoV G40V were subjected to IP with anti-HA magnetic beads (Bimake). The proteins were split by SDS-PAGE gel, visualized by a silver protein staining kit

(Thermo Fisher Scientific), and subjected to liquid chromatography tandem mass spectrometry (LC–MS/MS) analysis.

2.15 | Statistical analysis

Statistical analysis was performed with GraphPad Prism 8.0 (GraphPad Software) or SPSS 22.0 (IBM Analytics). Expression and clinical data of TCGA cohorts were downloaded from the website http://www.cbioportal.org/. Survival analysis was performed through the Kaplan–Meier method and compared with the log-rank test. For the transwell migration and wound-healing assays, *n* meant the number of biological replicates, and unpaired Student *t*-test was utilized to assess the statistical significance. All *p*-values were two sided, and *p*-values less than 0.05 were considered significant.

3 | RESULTS

3.1 | In vivo CRISPR screens targeting metastasis-related genes identify candidate pro-metastasis genes

Using our previous TNBC transcriptome database, a total of 440 genes were identified as metastasis-related genes according to differential expression between the high- and low-risk groups (Figure S1A). Subsequently, after transfecting the breast cancer MDA-MB-231 and LM2-4175 cell lines with the CRISPR library, we constructed a mouse tail vein metastasis model for in vivo screen (Figure 1A; Figure S1B,C). NGS was performed on the original plasmid library, day 0 cells, day 14 cells, lung metastases, and liver metastases. We then obtained the distribution of each sgRNA (Figure 1B; Figure S1D). The correlation coefficient between each sgRNA reading of cells was close to 1, indicating the plasmid library did not lose most sgRNA in the process, whereas in the lung and liver metastases, the correlation coefficient is close to 0 and the sgRNA exhibited diversity (Figure 1C).

We further utilized the MAGeCK algorithm to screen out genes that were negatively screened in lung metastases and liver metastases (Figure 1D). Among these genes, several well-known metastasis-associated genes were on the list of top-ranked genes, such as ITGB4, FN1, and CDK6.[19–21] We selected the top 50 genes ranked by mScore to analyze their prognosis in the FUSCC TNBC cohort. The high expression of most top genes indicated poor prognosis of TNBC (Figure 1E). Meanwhile, we conducted pathway analysis on the top 100 genes and found that pathways were mainly in changes of cell development and cell-matrix adhesion, and the RhoV gene studied in this research was closely related to these two pathways (Figure 1F).

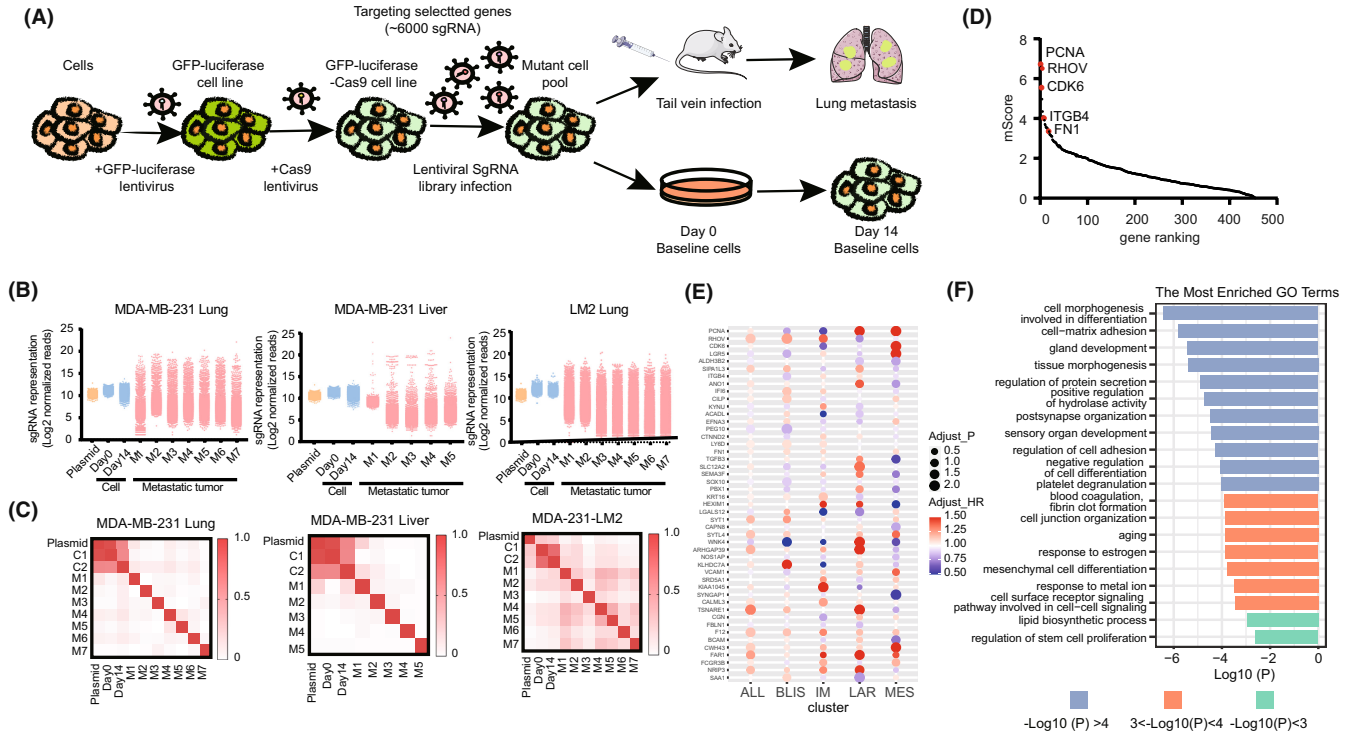

FIGURE 1 RNA-Seq derived metastasis-gene related library generation and in vivo CRISPR screen show genes associated with tumor metastasis. (A) Schematic representation of the CRISPR screen. (B), Scatterplots of normalized read counts for the library sgRNA. M1–M7 indicate the individual mice. (C) Pearson correlation coefficient in each group of the normalized sgRNA read counts. (D) Ranking of the genes according to their corresponding mScore value. (E) The prognostic predictive ability of the top 50 genes in the overall Fudan University Shanghai Cancer Center (FUSCC) triple-negative breast cancer (TNBC) and the four subtypes. The size of the dot indicates the hazard ratio (HR) value, and the color of the dot indicates the prognosis. (F) Gene ontology analysis of top-100 genes. *p*-values for each enriched functional category were calculated by the Fisher exact test. Different colors mean different ranges of *p*-values.

3.2 | RhoV is frequently upregulated in breast cancer and indicates a poor prognosis

RhoV ranked especially high in the overall ranking and separate ranking (Figure 1D, Figure 2A–C; Table S2), and there are few previous reports on its role in metastasis. Therefore, we selected RhoV for further research. In the CCLE database, RhoV was highly expressed in breast cancer (Figure S2A). Analysis of the methylation level of RhoV in all cancers also indicated that RhoV was specifically hypomethylated in breast cancer (Figure S2B). Furthermore, it showed that RhoV was highly expressed in TNBC compared with normal tissue (Figure 2D). Also, the expression of RhoV is higher in TNBC than non-TNBC in the TCGA cohort (Figure 2E).

We next explored the prognostic implications of RhoV in TNBC. The higher expression of RhoV in the FUSCC cohort predicted shorter disease-free survival (DFS) (Figure 2F, $p = 0.015$; Table S3). TNBC samples from the TCGA cohort also suggested the same result (Figure 2G, $p = 0.009$). In addition, the analyses derived from the Kaplan–Meier plots indicated high RhoV expression was correlated with poor DFS and overall survival in TNBC (Figure S3A). Clinically, the axillary lymph node metastasis of TNBC patients is one of the most important prognostic indicators. We found even in TNBC patients with negative axillary lymph node metastasis, higher expression of RhoV still indicated shorter DFS in the FUSCC database (Figure 2H, $p = 0.034$) and TCGA database (Figure 2I, $p = 0.017$). Similar results were obtained when distant metastasis-free survival was compared (Figure S3B). Meanwhile, the expression of RhoV increased as the lymph node staging increased in the FUSCC and TCGA TNBC cohort (Figure S3C; Table S4). Based on the above results, we believe RhoV has great clinical value as a prognostic indicator of TNBC.

3.3 | RhoV promotes metastasis of TNBC cells

RhoV belongs to the CDC42 subprotein family of the Rho protein family and has high sequence homology with CDC42. CDC42 could promote the formation of filopodia. Consistently, overexpression of RhoV and RhoV G40V (RhoV activated mutation) in MDA-MB-231 cells promoted filopodia formation (Figure S4A,B). As RhoV has no commercially available Western blot antibodies, we employed RT-PCR to verify the expression of RhoV after siRNA knockdown in MDA-MB-231 and HCC-70 cells (Figure S4C). Transwell migration and invasion experiments showed that cell migration ability decreased after knockdown of RhoV (Figure 3A,B). However, viability experiments indicated that knockdown of RhoV had no significant effect on the proliferation (Figure 3C). RhoV and RhoV G40V were further overexpressed in MDA-MB-231 and BT-549 cells. The level of cell migration and invasion increased significantly (Figure 3D,E). We also conducted a wound-healing assay and found that overexpression of RhoV and RhoV G40V promoted cell migration (Figure S4D). To further validate our result in vivo, we employed a lung metastasis model using MDA-MB-231 cells stably expressing shNC, shRhoV#1, and shRhoV#3 injected into the tail vein of NOD/SCID mice. Lung metastasis of shRhoV#1 and shRhoV#3 was significantly less compared with shNC (Figure 3F).

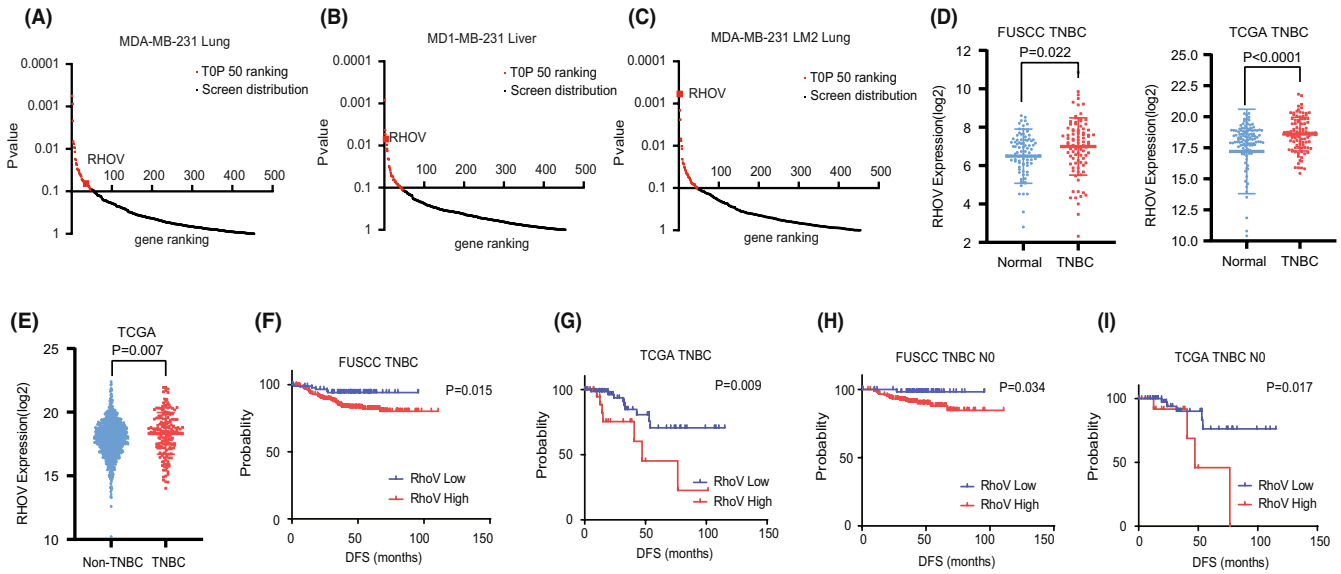

FIGURE 2 RhoV is associated with poor clinical outcome. (A–C) Ranking of RhoV according to *p*-value of the MAGeCK algorithm in MDA-MB-231 lung, MDA-MB-231 liver, and MDA-MB-231 LM2 lung metastatic foci. (D) Significant correlation between RhoV expression and triple-negative breast cancer (TNBC) tumor in both Fudan University Shanghai Cancer Center (FUSCC) and The Cancer Genome Atlas (TCGA) data sets. (E) RhoV expression between non-TNBC and TNBC in TCGA cohort. (F) Kaplan–Meier analysis of disease-free survival (DFS) using the FUSCC cohort. (G) Kaplan–Meier analysis of DFS using TCGA cohort. (H) Kaplan–Meier analysis of DFS in patients with negative lymph nodes using the FUSCC cohort. (I) Kaplan–Meier analysis of DFS in patients with negative lymph nodes using TCGA TNBC cohort. Values of *p* were calculated with the two-sided log-rank test.

Also, lung metastasis of overexpression of RhoV and RhoV G40V was more than that of the control group (Figure 3G). These results indicated that RhoV plays a key role in promoting metastasis of TNBC cells.

3.4 | GRB2 interacts with RhoV and regulates RhoV's tumor metastasis-promoting function

To investigate how RhoV affects TNBC migration, we conducted IP and LC–MS/MS to explore RhoV-interacting proteins. Common binding proteins of the rho family were detected like ARHGEF7, GIT1, and GIT2 (Figure 4A). Meanwhile, GRB2 was also detected, which is a downstream protein of receptor tyrosine kinase (RTK) and usually does not interact with rho family proteins (Figure 4A). We next successfully verified the binding of RhoV and GRB2 in HEK293T and MDA-MB-231 by IP analysis to pull down HA-tagged RhoV and RhoV G40V (Figure 4B,C). Furthermore, the anti-GRB2 antibody was used to pull down endogenous GRB2, which also verified the mutual binding of RhoV and GRB2 (Figure 4D). PAK1 is one of the most famous effector proteins of RhoV.[22] In HEK293 cells, RhoV/RhoV G40V and GRB2 were simultaneously overexpressed, and when GRB2 was overexpressed, the binding of RhoV G40V and PAK1 increased. It indicated GRB2 could promote the downstream activation of RhoV (Figure 4E). Meanwhile, in transwell experiments, we found knocking down GRB2 reversed the protumor migration phenotype caused by RhoV (Figure 4F). Similar results were obtained in the wound-healing assays in MDA-MB-231 and Hs-578T cells (Figure 4G).

3.5 | RhoV interacts with GRB2 through its N-terminal SH3 domain

PXXPXR is a common binding site of the SH3 domain of GRB2.[23] To confirm the binding site of RhoV and GRB2, we constructed mutant

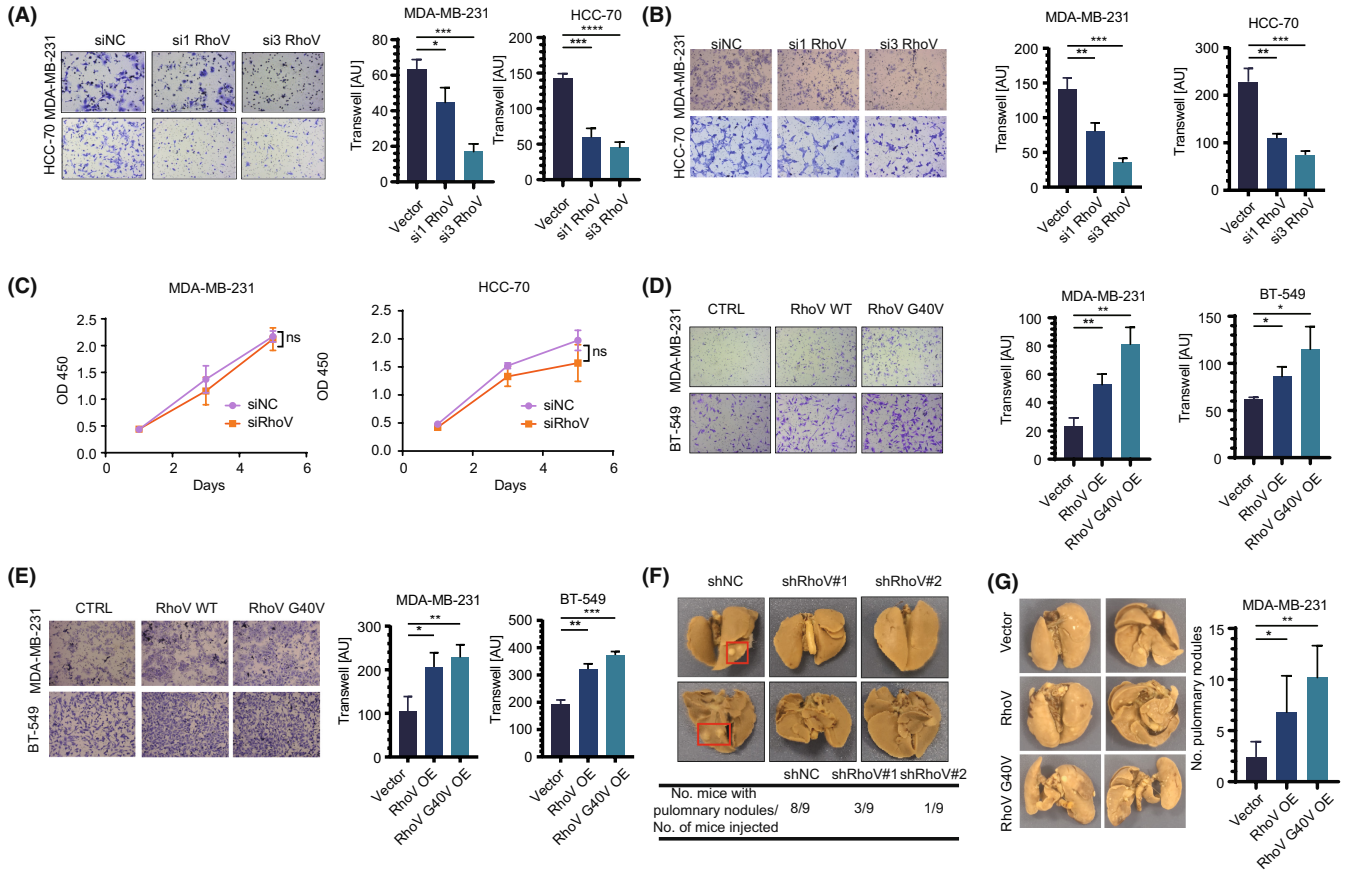

FIGURE 3 RhoV plays a role in triple-negative breast cancer (TNBC) metastasis. (A) MDA-MB-231 and HCC-70 cells were transiently transfected with small interfering RNA (siRNA) targeting RhoV. Transwell migration chamber assays were conducted to study changes in migration capacity ($n = 3$). The image (left) and quantitative analysis of the total invasive cells (right) are shown. (B) MDA-MB-231 and HCC-70 cells were transiently transfected with siRNA (small interfering RNA) targeting RhoV. Transwell invasion assays were conducted to study changes in invasion capacity ($n = 3$). (C) Cell viability assay of MDA-MB-231 and HCC-70 cells ($n = 3$). (D) Transwell migration assays of MDA-MB-231 and BT-549 cells transiently transfected with RhoV and RhoV G40V ($n = 3$). (E) Transwell invasion assays of MDA-MB-231 and BT-549 cells transiently transfected with RhoV and RhoV G40V ($n = 3$). (F) Representative images of lung metastasis of MDA-MB-231 cells stably expressing shNC, shRhoV#1, and shRhoV#3 injected into the tail vein of NOD/SCID mice ($n = 9$). (G) Representative images of lung metastasis of MDA-MB-231 cells stably expressing RhoV and RhoV G40V injected into the tail vein of NOD/SCID mice ($n = 5$).

plasmids of the PXXPXR domain at the N-terminal of RhoV (Figure 5A). In HEK293T cells, we overexpressed the mutant RhoV and GRB2, and the Co-IP experiment successfully verified that when the R (Arg, arginine) of the PXXPXR domain or the whole PXXPXR domain was deleted, RhoV could not bind with GRB2. Therefore, we concluded that RhoV interacts with GRB2 through its N-terminal PXXPXR domain. However, we also found deleting PXXPXR domain may affect the stability of the RhoV protein and lead to its degradation (Figure 5A). In transwell experiments we found that RhoV Mut4 (double arginine-deleted mutation) overexpression could not promote or even inhibited cell migration (Figure 5B). Similar phenotype results were obtained in wound-healing assays in MDA-MB-231 and Hs-578 T cells (Figure S4E). Knockdown of RhoV inhibits cell migration, and it can be rescued by overexpression of RhoV WT but not RhoV Mut4 (Figure 5C).

3.6 | Epidermal growth factor receptor interacts with RhoV through GRB2 and promotes downstream activation of RhoV

Epidermal growth factor receptor signaling cascade is a key regulator in cancer development. As we had proved that RhoV could bind with GRB2, we further wanted to explore whether RhoV could bind with EGFR, the upstream protein of GRB2.[24] Through the Co-IP experiment, we found that under the stimulation of EGF, RhoV could bind with p-EGFR (Figure 5D). We supposed that under the stimulation of EGF, p-EGFR interacted with GRB2, and further indirectly interacted with RhoV to activate RhoV and its downstream proteins. Then, we wanted to verify whether the interaction between RhoV and EGFR is dependent on GRB2. In Co-IP experiment, we demonstrated that

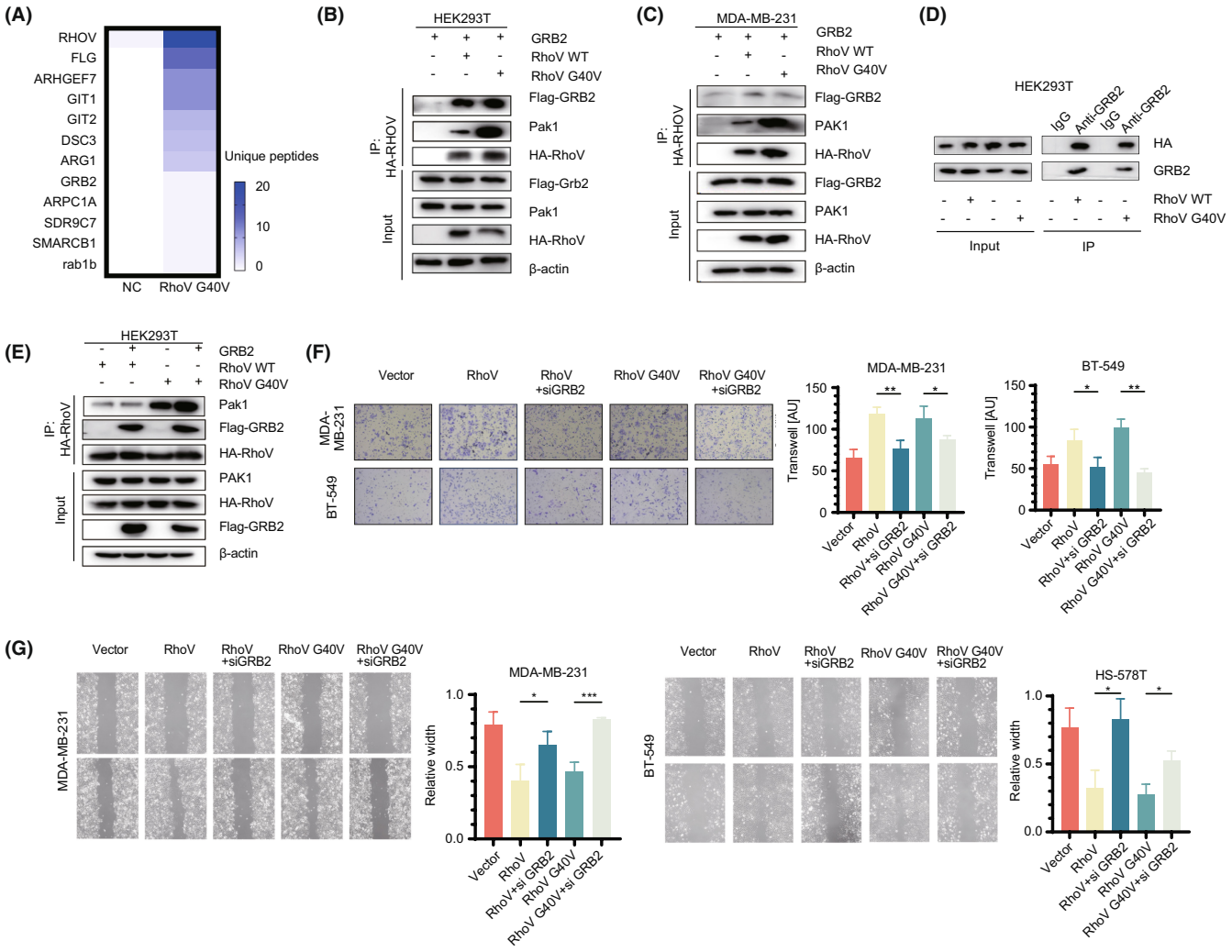

FIGURE 4 GRB2 interacts with RhoV and regulates RhoV's tumor migration-promoting effect. (A) Immunoprecipitation experiments on HEK-293 T-control and HA-RhoV-overexpressed protein samples were identified by mass spectrometry. The identified protein and relative abundances are shown by a heatmap. (B, C) His-GRB2 combined with CTRL, HA-RhoV- or HA-RhoV G40V-overexpressed HEK293T and MDA-MB-231 cells were immunoprecipitated by anti-HA magnetic beads. (D) HA-RhoV- or HA-RhoV G40V-transfected HEK293T cells were lysed and immunoprecipitated by anti-GRB2 antibody. (E) HA-RhoV- or HA-RhoV G40V-transfected HEK293T cells were transfected with or without GRB2. Cells were lysed and immunoprecipitated by anti-HA magnetic beads. (F) Cell migration ability was measured by the transwell chamber assays assay ($n = 3$). (G) Wound-healing assay for MDA-MB-231 and Hs-578 T cells transfected with RhoV and RhoV G40V with or without siGRB2.

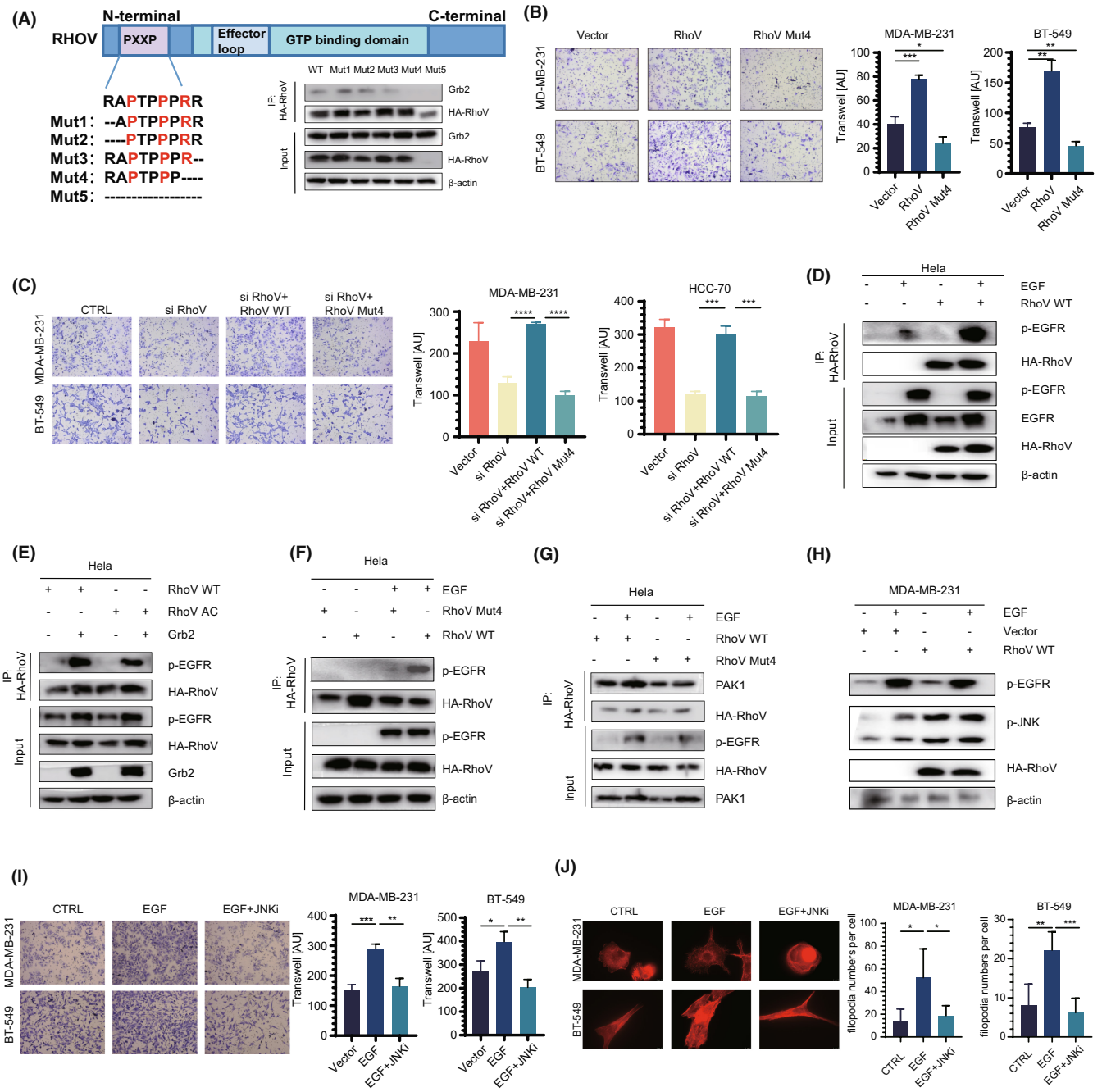

FIGURE 5 The EGFR/GRB2 axis promotes the downstream activation of RhoV. (A) CTRL or HA-tagged different RhoV mutants overexpressing HEK293T cells were immunoprecipitated with anti-HA magnetic beads and immunoblotted. (B) Cell with migration ability was measured by transwell chamber assays assay ($n = 3$). (C) Transwell migration assays of MDA-MB-231 and BT-549 cells transiently transfected with RhoV and RhoV Mut4 after transfection with siRNA targeting RhoV ($n = 3$). (D) HA-RhoV- or HA-RhoV G40V-transfected, serum-starved HeLa cells were stimulated with or without EGF. Cells were lysed and immunoprecipitated by anti-HA magnetic beads. (E) HA-RhoV- or HA-RhoV G40V-transfected (with or without GRB2), serum-starved HeLa cells were stimulated with or without EGF. Cells were lysed and immunoprecipitated by anti-HA magnetic beads. (F) RhoV- or RhoV Mut4-transfected, serum-starved HeLa cells were stimulated with or without EGF. Cells were lysed and immunoprecipitated by anti-HA magnetic beads. (G) HA-RhoV- or HA-RhoV Mut4-transfected, serum-starved HeLa cells were stimulated with or without EGF. Cells were lysed and immunoprecipitated by anti-HA magnetic beads. (H) Control vector- and HA-RhoV-transfected, serum-starved cells were stimulated with EGF. Cell lysates immunoblotted with indicated EGF-dependent signaling antibodies. (I) Transwell migration assays of MDA-MB-231 and BT-549 cells stimulated with or without EGF. JNK inhibitor was applied in EGF-stimulated cells. (J) Filamentous Actin was visualized with TRITC-conjugated phalloidin in MDA-MB-231 and BT-549 cells stimulated with or without EGF. JNK inhibitor was applied in EGF-stimulated cells.

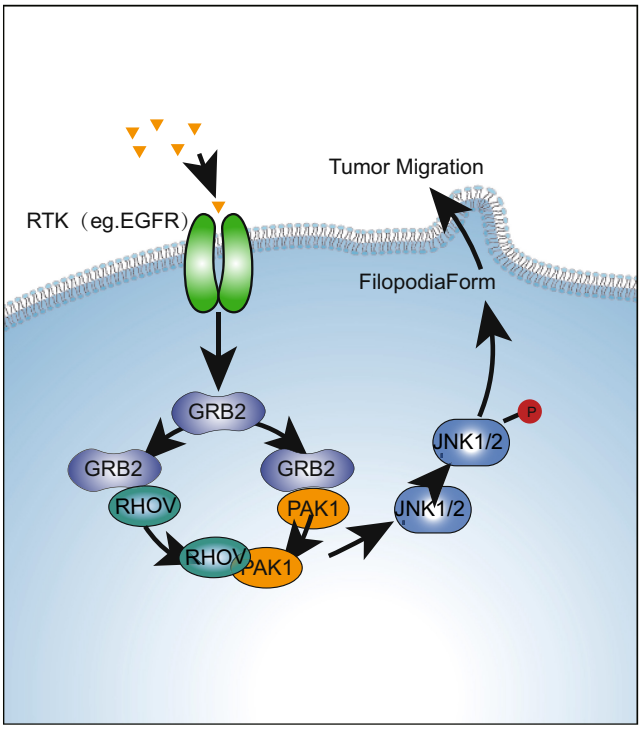

FIGURE 6 The mechanism pattern diagram of RhoV promoting triple-negative breast cancer (TNBC) metastasis.

GRB2 overexpression strongly improved the binding of RhoV and p-EGFR (Figure 5E). Also, we showed that RhoV Mut4 was unable to interact with p-EGFR, as this mutation failed to interact with GRB2 (Figure 5F). Therefore, we are convinced that RhoV could interact with EGFR through GRB2. Next, we investigated whether EGF could activate the downstream proteins of RhoV and selected the known downstream signal pathway PAK1-JNK1/2 for verification.[25] Apart from its nuclear functions, JNK also regulates the filopodia by phosphorylation of diverse cytoplasmic targets.[26] Under EGF stimulation, the binding ability of RhoV WT to PAK1 was significantly greater than RhoV Mut4, and the binding ability of RhoV WT to PAK1 was increased under the stimulation of EGF, while RhoV Mut4 was not (Figure 5G). Subsequently, we found that under the stimulation of EGF and overexpression of RhoV, the expression of p-JNK increased in the MDA-MB-231 cell line, but there was no significant change in Hela cells (Figure 5H, Figure S4F), possibly indicating that RhoV plays a role specifically in breast cancer cells. JNK inhibitor could suppresses EGF-induced and RhoV-overexpression cell migration and filopodia formation in MDA-MB-231 and BT-549 (Figure 5I,J, Figure S4G,H).

Based on the above data, we concluded the specific role of RhoV in promoting TNBC metastasis (Figure 6). Under the stimulation of EGF, the EGFR is activated. The p-EGFR further recruits the adaptor protein GRB2. In this process, GRB2 acts as a platform, enabling RhoV and PAK1 to enrich to the signal activation site.[27] This effect greatly improves the combination probability of two proteins, activates the downstream PAK1-JNK1/2 signaling pathway, promotes the formation of tumor filopodia, and further promotes the metastasis of TNBC cells.

4 | DISCUSSION

In this research, we utilized an unbiased genetic screen to explore TNBC metastasis-related genes. We generated a small customized CRISPR-Cas9 library and established a mouse model of metastasis from TNBC cell lines transfected with the library, which helped us find out RhoV promoting TNBC metastasis.

RhoV belongs to the atypical Rho family GTPases, which are poorly understood.[28] RhoV induces the formation of lamellipodia and is located in the adhesion spots of endothelial cells.[29] RhoV is reported to be expressed in the embryos of *Xenopus laevis* and plays an important role in neural crest cells differentiation.[30] In zebrafish embryos, RhoV regulates the localization of E-cadherin at adhesion junctions through the activation of βPIX and Pak1.[31] Previous research has described RhoV plays an essential role in many cellular functions, including cytoskeleton formation, cell polarity, cell proliferation, and so on.[32,33] Importantly, RhoV activity has also been implied to be related with cellular transformation.[32]

However, the particular mechanisms underlying RhoV activation are still poorly understood. Here, we firstly demonstrated that RhoV functionally and physically couples with activated EGFR by GRB2. EGFR is an important member of the RTK family. After ligand binding, EGFR dimerizes and triggers downstream signaling activity, including phosphatidylinositol 3-kinase, protein kinase C (PKC), and mitogen-activated protein kinase (MAPK).[34] The adaptor molecular GRB2, which contains an SH2 domain with two flanking SH3 domains, plays important roles in these processes.[35] The SH2 domain binds the phosphotyrosine residues of EGFR,[36] and the SH3 domains can recognize proline-rich domains like those found in SOS, the exchange factor of Ras GTP. Thus, GRB2 links EGFR to downstream signaling and further degradation.[35]

Our results not only imply a unique activation mechanism of RhoV via N-terminal-mediated SH3 interaction but also find a previously undiscovered role for RhoV in regulating EGF signaling and show an additional possible mechanism by which RhoV can promote metastasis.

One limitation in the present study should be mentioned. Although we found that RhoV is specifically and highly expressed in breast cancer, this article does not fully clarify the physiological functions of RhoV in breast cancer cells. Therefore, we believe that how RhoV functions in breast cancer cells still needs to be further explored.

AUTHOR CONTRIBUTIONS

Z.-M.S. and X.H. joined in the design of the study. M.-L.J., Y.G., and P.J. performed the experiments. M.-L.J. and Y.G. performed statistical analysis of the data. M.-L.J., Y.G., P.J., X.H., and Z.-M.S. wrote, reviewed, and/or revised the manuscript. X.H. and Z.-M.S. supervised the study.

ACKNOWLEDGMENTS

We are appreciated of TCGA Research Network for the data analyzed.

FUNDING INFORMATION

This work was supported by grants from the National Natural Science Foundation of China (81572583, 81502278, 82103369, and 82202995) and China Postdoctoral Science Foundation (2022M710757).

ETHICS STATEMENT

Approval of the research protocol by an Institutional Reviewer Board: Not applicable.

Informed Consent: Not applicable.

Registry and the Registration No. of the study/trial: Not applicable.

Animal Studies: Not applicable.

CONFLICT OF INTEREST STATEMENT

The authors declare that they have no competing interests.

ORCID

Ming-Liang Jin https://orcid.org/0000-0003-3465-2392
Xin Hu https://orcid.org/0000-0002-8160-8362
Zhi-Ming Shao https://orcid.org/0000-0001-8781-2455

REFERENCES

1. Dent R, Trudeau M, Pritchard KI, et al. Triple-negative breast cancer: clinical features and patterns of recurrence. *Clin Cancer Res*. 2007;13:4429-4434. doi:10.1158/1078-0432.Ccr-06-3045
2. Siegel R, Miller K, Fuchs H, Jemal A. Cancer statistics, 2021. *CA Cancer J Clin*. 2021;71:7-33. doi:10.3322/caac.21654
3. Al-Mahmood S, Sapiezynski J, Garbuzenko O, Minko T. Metastatic and triple-negative breast cancer: challenges and treatment options. *Drug Deliv Transl Res*. 2018;8:1483-1507. doi:10.1007/s13346-018-0551-3
4. Gerratana L, Fanotto V, Bonotto M, et al. Pattern of metastasis and outcome in patients with breast cancer. *Clin Exp Metastasis*. 2015;32:125-133. doi:10.1007/s10585-015-9697-2
5. Zeichner S, Terawaki H, Gogineni K. A review of systemic treatment in metastatic triple-negative breast cancer. *Breast Cancer*. 2016;10:25-36. doi:10.4137/bcbcr.S32783
6. Manguso R, Pope HW, Zimmer MD, et al. In vivo CRISPR screening identifies Ptpn2 as a cancer immunotherapy target. *Nature*. 2017;547:413-418. doi:10.1038/nature23270
7. Faure S, Fort P. Atypical RhoV and RhoU GTPases control development of the neural crest. *Small GTPases*. 2015;6:174-177. doi:10.1080/21541248.2015.1025943
8. Orgaz J, Herraiz C, Sanz-Moreno V. Rho GTPases modulate malignant transformation of tumor cells. *Small GTPases*. 2014;5:e29019. doi:10.4161/sgtp.29019
9. Fritz G, Kaina B. Rho GTPases: promising cellular targets for novel anticancer drugs. *Curr Cancer Drug Targets*. 2006;6:1-14. doi:10.2174/1568009610606010001
10. Jaffe A, Hall A. Rho GTPases: biochemistry and biology. *Annu Rev Cell Dev Biol*. 2005;21:247-269. doi:10.1146/annurev.cellbio.21.020604.150721
11. Rossman K, Der C, Sondek J. GEF means go: turning on RHO GTPases with guanine nucleotide-exchange factors. *Nat Rev Mol Cell Biol*. 2005;6:167-180. doi:10.1038/nrm1587
12. Tcherkezian J, Lamarche-Vane N. Current knowledge of the large RhoGAP family of proteins. *Biol Cell*. 2007;99:67-86. doi:10.1042/bc20060086
13. Barretina J, Caponigro G, Stransky N, et al. The cancer cell line encyclopedia enables predictive modelling of anticancer drug sensitivity. *Nature*. 2012;483:603-607. doi:10.1038/nature11003
14. Ghandi M, Huang FW, Jané-Valbuena J, et al. Next-generation characterization of the cancer cell line encyclopedia. *Nature*. 2019;569:503-508. doi:10.1038/s41586-019-1186-3
15. Jiang Y, Suo C, Shi J, et al. Genomic and transcriptomic landscape of triple-negative breast cancers: subtypes and treatment strategies. *Cancer Cell*. 2019;35:428-440.e5. doi:10.1016/j.ccell.2019.02.001
16. Shalem O, Sanjana NE, Hartenian E, et al. Genome-Scale CRISPR-Cas9 Knockout Screening in Human Cells. *Science*. 2014;343:84-87. doi:10.1126/science.1247005
17. Li W, Xu H, Xiao T, et al. MAGeCK enables robust identification of essential genes from genome-scale CRISPR/Cas9 knockout screens. *Genome Biol*. 2014;15:554. doi:10.1186/s13059-014-0554-4
18. Hu X, Kim JA, Castillo A, Huang M, Liu J, Wang B. NBA1/MERIT40 and BRE interaction is required for the integrity of two distinct deubiquitinating enzyme BRCC36-containing complexes. *J Biol Chem*. 2011;286:11734-11745. doi:10.1074/jbc.M110.200857
19. Ruan S, Lin M, Zhu Y, et al. Integrin β4-targeted cancer immunotherapies inhibit tumor growth and decrease metastasis. *Cancer Res*. 2020;80:771-783. doi:10.1158/0008-5472.Can-19-1145
20. Glasner A, Levi A, Enk J, et al. NKp46 receptor-mediated interferon-γ production by natural killer cells increases fibronectin 1 to Alter tumor architecture and control metastasis. *Immunity*. 2018;48:107-119.e104. doi:10.1016/j.immuni.2017.12.007
21. Zhang Z, Li J, Ou Y, et al. CDK4/6 inhibition blocks cancer metastasis through a USP51-ZEB1-dependent deubiquitination mechanism. *Signal Transduct Target Ther*. 2020;5:25. doi:10.1038/s41392-020-0118-x
22. Korobko I, Shepelev M. Mutations in the effector domain of RhoV GTPase impair its binding to Pak1 protein kinase. *Mol Biol*. 2018;52:692-698. doi:10.1134/s0026898418040092
23. Kami K. Diverse recognition of non-PxxP peptide ligands by the SH3 domains fro m p67phox, Grb2 and Pex13p. *EMBO J*. 2002;21:4268-4276. doi:10.1093/emboj/cdf428
24. Buday L, Downward J. Epidermal growth factor regulates p21ras through the formation of a complex of receptor, Grb2 adapter protein, and Sos nucleotide exchange factor. *Cell*. 1993;73:611-620. doi:10.1016/0092-8674(93)90146-h
25. Zhou Y, Xie Y, Li T, et al. P21-activated kinase 1 mediates angiotensin II-induced differentiation of human atrial fibroblasts via the JNK/c-Jun pathway. *Mol Med Rep*. 2021;23:27. doi:10.3892/mmr.2021.11846
26. Brunt L, Greicius G, Rogers S, et al. Vangl2 promotes the formation of long cytonemes to enable distant Wnt/β-catenin signaling. *Nat Commun*. 2021;12:2058. doi:10.1038/s41467-021-22393-9
27. Puto LA, Pestonjamasp K, King CC, Bokoch GM. p21-activated kinase 1 (PAK1) interacts with the Grb2 adapter protein to couple to growth factor signaling. *J Biol Chem*. 2003;278:9388-9393. doi:10.1074/jbc.m208414200
28. Aspenström P, Ruusala A, Pacholsky D. Taking rho GTPases to the next level: the cellular functions of atypical rho GTPases. *Exp Cell Res*. 2007;313:3673-3679. doi:10.1016/j.yexcr.2007.07.022
29. Aspenström P, Fransson A, Saras J. Rho GTPases have diverse effects on the organization of the Actin filament system. *Biochem J*. 2004;377:327-337. doi:10.1042/bj20031041
30. Guémar L, de Santa Barbara P, Vignal E, Maurel B, Fort P, Faure S. The small GTPase RhoV is an essential regulator of neural crest induction in Xenopus. *Dev Biol*. 2007;310:113-128. doi:10.1016/j.ydbio.2007.07.031
31. Tay H, Ng Y, Manser E. A vertebrate-specific Chp-PAK-PIX pathway maintains E-cadherin at adherens junctions during zebrafish epiboly. *PLoS One*. 2010;5:e10125. doi:10.1371/journal.pone.0010125
32. Aronheim A, Broder YC, Cohen A, Fritsch A, Belisle B, Abo A. Chp, a homologue of the GTPase Cdc42Hs, activates the JNK pathway

and is implicated in reorganizing the Actin cytoskeleton. *Curr Biol*. 1998;8:1125-1128. doi:10.1016/s0960-9822(98)70468-3
33. Shepelev M, Chernoff J, Korobko I. Rho family GTPase Chp/RhoV induces PC12 apoptotic cell death via JNK activation. *Small GTPases*. 2011;2:17-26. doi:10.4161/sgtp.2.1.15229
34. Nicholson R, Gee J, Harper M. EGFR and cancer prognosis. *Eur J Cancer*. 2001;37:S9-S15. doi:10.1016/s0959-8049(01)00231-3
35. Rozakis-Adcock M, Fernley R, Wade J, Pawson T, Bowtell D. The SH2 and SH3 domains of mammalian Grb2 couple the EGF receptor to the Ras activator mSos1. *Nature*. 1993;363:83-85. doi:10.1038/363083a0
36. Lowenstein E, Daly RJ, Batzer AG, et al. The SH2 and SH3 domain-containing protein GRB2 links receptor tyrosine kinases to ras signaling. *Cell*. 1992;70:431-442. doi:10.1016/0092-8674(92)90167-b

SUPPORTING INFORMATION

Additional supporting information can be found online in the Supporting Information section at the end of this article.

How to cite this article: Jin M-L, Gong Y, Ji P, Hu X, Shao Z-M. In vivo CRISPR screens identify RhoV as a pro-metastasis factor of triple-negative breast cancer. *Cancer Sci*. 2023;114:2375-2385. doi:10.1111/cas.15783